JOURNAL OF GUIDANCE, CONTROL, AND DYNAMICS
Vol. 16, No. 1, January-February 1993

Application of the Global Positioning System for Hermes Rendezvous Navigation

B. A. C. Ambrosius,* E. T. Hesper,† and K. F. Wakker‡
Delft University of Technology, Delft, The Netherlands

A study of the application of the global positioning system (GPS) for precise real-time relative orbit determination during rendezvous and docking operations in low Earth orbit has been performed. It is a first attempt to analyze this complex problem, in which the relative navigation accuracy during the homing and closing phase of a typical rendezvous mission between the European space plane Hermes and the Columbus Free Flying Laboratory has been investigated. Results are presented of a covariance analysis of a hypothetical on-orbit real-time data processing system, based on Kalman filtering of pseudorange observations acquired by GPS receivers onboard the two spacecraft. The so-called reduced-dynamic technique was applied for the orbit determination of both spacecraft. A method is described to derive the relative position and velocity errors from the absolute state-vector covariances. Two data processing concepts have been investigated. It is shown that using only observations of GPS satellites commonly visible from both rendezvouz spacecraft gives much better results than when all observations are used. Overall, the results indicate that accurate rendezvous navigation using GPS only is quite feasible.

Introduction

WITH the coming of the space station era, a large increase in the number of rendezvous and docking (RVD) missions in low Earth orbit (LEO) is anticipated. Because of this increase, current methods of monitoring and controlling the complex orbital operations for these missions from the ground are not feasible anymore. Therefore, it is necessary to move the emphasis in the design and planning of RVD missions toward a decreased dependence on ground facilities. The first step toward increased autonomy for RVD missions is the development of reliable onboard relative position and velocity determination techniques. In this case, the Navigation Satellite by Timing and Ranging Global Positioning System (NAVSTAR/GPS) is expected to provide the primary tool for most onboard navigation applications in RVD missions.

A typical example of such a mission is the servicing of the European Columbus Free Flying Laboratory (CFFL) by the Hermes space plane, in which CFFL is the passive "target" spacecraft and Hermes the active "chaser." An overview of the requirements and concepts of this mission are presented in Ref. 1. For this study, it has been assumed that both spacecraft are equipped with a GPS receiver, able to perform observations of all GPS satellites in view, whereas CFFL is supposed to be able to transmit its GPS data to Hermes. Suitable processing should then enable Hermes to determine its position and velocity relative to CFFL autonomously without any other information. Figure 1 shows a schematic representation of the problem.

The purpose of the study presented in this paper was to investigate the feasibility of this concept and to obtain an impression of the achievable relative navigation accuracy. Therefore, a covariance analysis was performed of the data reduction problem covering the homing and closing phases of the mission, during which Hermes approaches CFFL from a distance of about 1000 km to less than 100 m. The work described in this paper is partially based on two earlier studies.[2,3]

At the time we conducted our investigations, only a few publications on this topic were available. Reference 4 describes the concept of statistical covariance error analysis, applied to the problem of absolute navigation of the Space Shuttle with the aid of GPS. Our study can be considered as an extension of that work to the field of relative navigation. In Ref. 5, a theory is developed describing the characteristics of the GPS pseudorange and phase measurement data and a Kalman filter for onboard relative state-vector determination of rendezvous space vehicles. The usefulness of this method is limited to relative distances of less than 20 km, however. A similar approach was adopted in Ref. 6, which also presents some numerical results of deterministic simulations involving a "truth" model based on the Clohessy-Willshire equations for relative motion. Finally, another Monte Carlo-type simulation study is presented in Ref. 7, in which a simple parameter model with only eight state variables was used to estimate the orbital elements and a clock bias and drift from undifferenced pseudorange measurements. The relative positioning accuracy achieved using S-code measurements was 20 m in each axis.

In contrast with earlier studies,[6,7] we introduced the so-called reduced-dynamic technique[8] for the orbit determination of the rendezvous vehicles, in which the number of state parameters is expanded with three stochastic acceleration parameters for both spacecraft. They serve to absorb the unmodeled perturbation errors, which are primarily caused by the simplified dynamic models that are used in real-time navigation algorithms. This method allows a more realistic incorporation of the model errors than simply adding white noise to the velocity covariances during the time-update step.

Furthermore, two different data processing concepts have been considered in this study. The first involves differential navigation, in which the relative state vector is derived from the absolute navigation solution of both spacecraft, computed independently from the data of all available GPS satellites. The other concept is based on the processing of so-called single-difference observations. These are defined as the differences between pairs of pseudorange measurements of the same GPS satellite, taken simultaneously by the receivers on both spacecraft. In this case, the navigation solutions of both spacecraft can be derived concurrently and may be differenced, as in the first concept, or the relative solution may be obtained directly. In practice, there are some differences between both concepts when applied for real-time onboard relative positioning. In the first case, both vehicles need to be able

Received Nov. 15, 1990; revision received Jan. 10, 1992; accepted for publication March 13, 1992.

*Associate Professor, Faculty of Aerospace Engineering. Kluyverweg 1.
†Research Scientist, Faculty of Aerospace Engineering.
‡Professor, Faculty of Aerospace Engineering.

to perform their own orbit determination, and at least one of them must transfer the solutions to the other spacecraft. In the other case, the raw measurements must be transferred to one of the spacecraft, most likely the active one, which will use them to compute the relative position and velocity.

In the first part of this paper, we describe a method to derive relative error estimates from absolute state-vector covariances. It was developed because the software that we used for our analysis did not have the capability to compute the relative covariances directly. The second part elaborates on the adopted filter model, the mission scenario, and the error model used in the actual covariance analysis. Finally, some results are also presented in which the effects of limited visibility, reduced GPS constellation, data gap, and data quality are highlighted.

Since this study represents a first effort in this field, the analysis was restricted in many respects. In the first place, only pseudorange measurements were considered, in particular, the S-code type, which has the lowest precision. The main motivation for this was that this data type is the primary observable of the GPS receiver, which was already planned as part of the payload of CFFL. Obviously, the performance can be improved considerably by using P-code data or by adding phase observations. Furthermore, selective availability (SA) and antispoofing (AS) were not considered in the analysis. The effects of ionospheric refraction were also not considered. In addition, the models for some of the other effects were rather primitive. On the other hand, the assumptions for model errors and measurement precision are probably somewhat conservative. Still, we feel that the analysis presented in this paper gives a good impression of the overall performance of a realtime rendezvous navigation system based on GPS.

Determination of the Total Relative Uncertainties

The error analyses in this study were performed using the Orbit Analysis and Simulation Software (OASIS), developed at the Jet Propulsion Laboratory (JPL) for covariance analysis of point positioning and orbit determination problems, in particular, for those involving GPS.[9] It utilizes a Kalman filter for the parameter estimation. The data types that can be handled are many and include the various (differenced) kinds of GPS measurements, such as pseudorange and carrier phase. An interesting feature is that, except for the orbital parameters, all other parameters can be treated as stochastic variables. The covariance analysis also incorporates the so-called consider analysis of unestimated model parameters. This is a technique to study the effects of model errors other than data noise on the covariances of the filtered state estimates. It is predicated on the assumption that the consider parameters are simply bias parameters (e.g., atmospheric drag, gravity, GPS satellite position and velocity, etc.) that are not included in the set of estimated parameters. Furthermore, it is assumed that the consider parameters are not correlated with the estimated parameters. Consequently, the total covariance is equal to the sum of the contributions of both the estimated and the unestimated (consider) parameters given by

$$P_{\text{tot}} = \hat{P} + SP_cS^T \tag{1}$$

where $\hat{P}$ is the filter noise covariance matrix that represents the data noise errors, S is the sensitivity matrix that relates the consider parameters to the estimated parameters, and P_c is the diagonal covariance matrix for the consider parameters. However, in Ref. 10 it is shown that the actual total covariances can become much smaller than those obtained from Eq. (1), when possible correlations between the estimated parameters and the consider parameters are taken into account.

OASIS is not able to determine the relative position and velocity covariances of two spacecraft directly, but it computes the absolute position and velocity covariances of the individual satellites. Thus, to study the relative navigation errors, it was necessary to develop a method to derive the relative covariances from the absolute covariances in a postprocessing of the OASIS results. This method involves two steps, a transformation of the filter noise covariance matrix and a transformation of the sensitivity matrix. In the following discussion, these two steps will be described in more detail.

Relative Filter Noise Covariances

Although in practice the individual navigation solutions may be computed independently by the GPS receivers onboard the two spacecraft, in OASIS all parameters are estimated simultaneously. Assuming, for simplicity, that only the position and velocity components of both satellites are estimated, the filter noise covariance matrix of the estimated parameters has the form

$$\hat{P} = \begin{array}{c} \\ x_c \\ y_c \\ z_c \\ \cdot \\ \cdot \\ \cdot \\ \dot{z}_t \end{array} \begin{array}{c} \begin{array}{ccccc} x_c & y_c & z_c & \cdots & \dot{z}_t \end{array} \\ \left[\begin{array}{ccccc} \hat{P}(1,1) & \hat{P}(1,2) & \hat{P}(1,3) & & \hat{P}(1,12) \\ & \hat{P}(2,2) & \hat{P}(2,3) & & \hat{P}(2,12) \\ & & \hat{P}(3,3) & & \hat{P}(3,12) \\ & & & & \\ & & & & \\ & & & & \\ & & & & \hat{P}(12,12) \end{array} \right] \end{array} \tag{2}$$

where x_c, y_c, z_c, $\dot{x}_c$, $\dot{y}_c$, $\dot{z}_c$ and x_t, y_t, z_t, $\dot{x}_t$, $\dot{y}_t$, $\dot{z}_t$ denote the position and velocity components of the chaser and the target, respectively. The (co)variances of the relative position and velocity of the chaser with respect to the target simply follow from the expectations E of the differences. The expectation of the covariance of the relative position components x and y, for example, is given by

$$E[(x_c - x_t)(y_c - y_t)^T] = E(x_cy_c) - E(x_cy_t) - E(x_ty_c) + E(x_ty_t) \tag{3}$$

From this it can be seen easily that the covariance matrix of the relative state vector is obtained from

$$\hat{P}_r(i, k) = \hat{P}(i, k) - \hat{P}(i + 6, k) - \hat{P}(i, k + 6) + \hat{P}(i + 6, k + 6) \tag{4}$$

where $\hat{P}_r$ is the 6×6 matrix of the relative filter noise covariances (i, $k = 1, \ldots, 6$). It is pointed out that, when undifferenced pseudoranges are used as data type—simulating independent processing of the observations onboard both spacecraft—the off-diagonal elements in the matrix $\hat{P}$, representing the covariances between the state-vector components of the two satellites, will be zero. In that case, Eq. (4) reduces to

$$\hat{P}_r(i, k) = \hat{P}(i, k) + \hat{P}(i + 6, k + 6) \tag{5}$$

Relative Sensitivities

The contributions of the errors in the consider parameters to the total covariance are expressed by the sensitivity covariance matrix, given by

$$P_S = SP_cS^T \tag{6}$$

It should be realized that P_S is actually a combination of many similar matrices, one for each consider parameter. This is important, because that is the reason why it is possible to investigate the effect of each individual consider parameter. In principle, the relative sensitivity covariance matrix P_{Sr} can be derived from the matrix P_S, using the same procedure described previously for the filter noise covariances. However, it can be shown[10] that the same result is obtained when the relative sensitivities are computed first and subsequently substituted in Eq. (6). This approach is more efficient from a computational point of view.

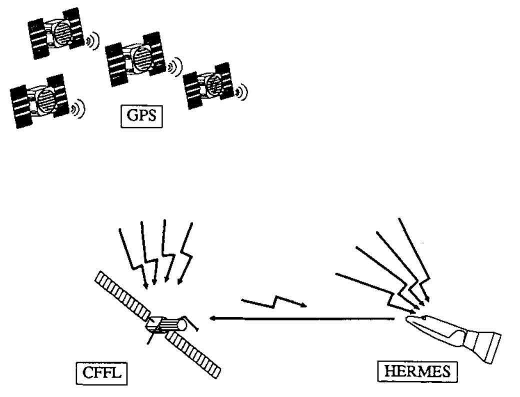

Fig. 1 Schematic representation of Hermes approaching the CFFL, while both are tracking the GPS signals.

Assuming again, for simplicity, that only the position and velocity vectors of two spacecraft are estimated simultaneously in the filter, the sensitivity matrix has the form

$$S = \begin{bmatrix} S(1,1) & S(1,2) & S(1,3) & \dots & S(1,n_c) \\ S(2,1) & S(2,2) & S(2,3) & & S(2,n_c) \\ S(3,1) & S(3,2) & S(3,3) & & S(3,n_c) \\ \cdot & & & & \\ \cdot & & & & \\ \cdot & & & & \\ S(12,1) & S(12,2) & S(12,3) & & S(12,n_c) \end{bmatrix} \tag{7}$$

where n_c is the number of consider parameters. The relative sensitivities are now simply obtained by subtracting the sensitivities of the corresponding elements of the state vectors of both satellites, according to

$$S_r(i,j) = S(i,j) - S(i+6,j) \tag{8}$$

where S_r is the $6 \times n_c$ relative sensitivity matrix ($i = 1, \dots, 6$, and $j = 1, \dots, n$). The relative sensitivity covariance matrix then follows from

$$P_{Sr} = S_r P_c S_r^T \tag{9}$$

Finally, it is mentioned that the actual implementation of this method was somewhat more complicated, due to the requirement to interface the algorithm with the OASIS software. Also, an additional transformation was added to present the results in a relative coordinate system, which makes it easier to interpret them.

Filter Strategy

In general, accurate orbit determination of a low-orbit satellite is quite complicated, because all kinds of effects perturbing the satellite's orbit have to be modeled very accurately. Especially in the case of sparse observation data, which is typical for ground-based tracking, the orbit needs to be propagated accurately between observation times. This requires detailed and complex models, for instance, for the Earth's gravity field, which would be prohibitive for real-time on-orbit application. Using simplified models introduces errors, which may lead to divergence of the solution. In any case, the accuracy of the orbital fit will never become better than the accuracy of the models. This limitation can be avoided, however, by exploiting the unique characteristics of the GPS system. It provides the capability to obtain multidirectional high-quality (pseudo)range observations continuously and at a high rate. In essence, this allows a user to make an independent geometric position determination at each measurement time, without the need of complex dynamical models. However, for moving users this is not the ideal method, because it does not provide velocity information and will lead to an interruption of the positioning capability if there is a temporary loss of data. Therefore, it is preferred to filter the observations, which does enable velocity determination. Besides, filtering has the added advantage of improving the accuracy of the solutions. However, this would still require the model, used to link dynamically the positions of the user at successive observation times, to be very accurate. Otherwise, the filter will become unstable, unless the errors are accounted for in the statistical model of the orbit determination process.

The simplest solution is to add white noise to the filter covariances during each time-update step. This is a primitive approach, since it destroys the correlations between the various estimated parameters and does not provide a good representation of the real model errors. A better way is to add three process noise parameters to the set of estimated parameters, representing fictitious accelerations in three orthogonal directions. These will absorb the effects of the unmodeled perturbing forces if their stochastic properties are tuned correctly. The accelerations are modeled as first-order exponentially time-correlated Gauss-Markov processes, which are characterized by a correlation time τ and a steady-state sigma σ_p. The change of the variance P_j of a process noise parameter from time t_j to t_{j+1} then is

$$P_{j+1} = m^2 P_j + \sigma^2 \tag{10}$$

where σ^2 is given by

$$\sigma^2 = (1 - m^2)\sigma_p^2 \tag{11}$$

with

$$m = \exp - \left(\frac{t_{j+1} - t_j}{\tau} \right) \tag{12}$$

In this approach, the values of the stochastic process noise parameters τ and σ_p determine the nature of the effective orbit determination strategy. If $\tau \to 0$ and $\sigma_p \to \infty$, the strategy is nondynamic or purely geometric, because the information from the previous measurement time is weighted down to zero in the time-update step, before the next measurement is processed. Conversely, the strategy is purely dynamic if $\tau \to \infty$ and $\sigma_p \to 0$. In that case the accreted dynamic information is

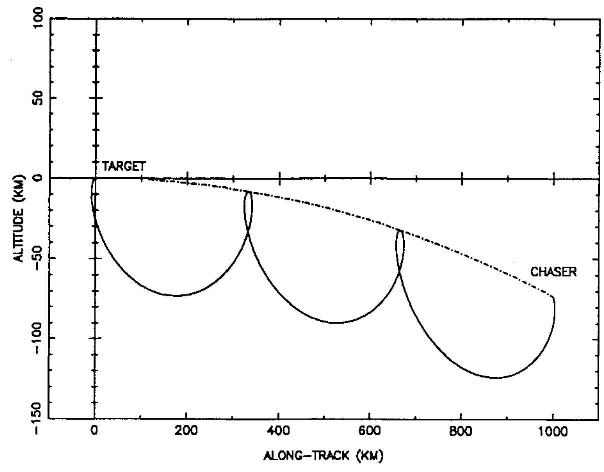

Fig. 2 Relative two-dimensional trajectory of the chaser with respect to the target, located at the intersection of the axes, in a reference frame corotating with the target. The dashed line represents the outline of a circular orbit with the radius of the target's orbit in this reference frame.

Table 1 Orbit and area-to-mass-ratio of the satellites

	GPS	Hermes Before maneuver	Hermes After maneuver	CFFL
Semimajor axis, km	26,560	6878	6843	6878
Eccentricity	0	0	0.0052	0
Inclination, deg	55	28.5	28.5	28.5
Right ascension of ascending node, deg	various	0	0	0
Argument of perigee, deg	0	0	118.2	0
Mean anomaly, deg	various	0	N.A.	8.33
Orbital period, min	718	94.6	93.8	94.6
Area-to-mass ratio, m/kg	N.A.	0.00476	0.00476	0.01

retained, since the variance of the acceleration parameters is not changed during the time update. The reduced-dynamic technique, which was applied in this study, combines the advantages of both extreme strategies by a proper choice of τ and σ_p. In Ref. 8 a more detailed discussion of this technique is presented.

Apart from the state vectors of both satellites and these extra acceleration parameters, the clocks onboard the rendezvous vehicles are also treated as estimated parameters. This is because these clocks will generally drift with respect to the GPS time system. Since the behavior of a clock can be characterized as a stochastic process, the clocks were modeled as random walk parameters.

Mission Profile and Error Model

In the actual error analyses, the originally planned 18-GPS satellite configuration was used, with three satellites, equally spaced in distance by 120 deg, in each of six orbital planes. The orbital planes are inclined 55 deg to the equator and are uniformly spaced in longitude by 60 deg. The phasing angle between the GPS satellites in different planes is 40 deg. The currently planned baseline configuration is 21 satellites plus three active spares, which means that the actual tracking coverage of potential RVD missions using GPS will be better.

The selected orbit parameters of Hermes and Columbus are based on the planned orbit of the latter. A simplified mission scenario was adopted, using a single trajectory to represent the last part of the transfer phase followed by the homing and closing phase of the rendezvous. In this scenario, both spacecraft are initially in identical circular orbits, with the chaser trailing by about 1000 km. At 78 min in this mission, the chaser is maneuvered into an elliptical orbit with a 70-km lower perigee, changing the orbital period such that it will catch up with the target in exactly three revolutions. The maneuver consists of a velocity change of about 20 m/s opposite to the direction of flight. Table 1 lists the orbital parameters of the various spacecraft involved in this study. For Hermes the parameters before and after the maneuver are listed. Also, the area-to-mass ratios of Hermes and Columbus are presented, as they have been used in the modeling of the drag effects. Figure 2 shows the trajectory of the chaser relative to the target after the maneuver in a corotating reference frame with its origin at the target.

The total mission time covered by the analyses is 6 h. The first 30 min of this period are reserved to allow the solutions of the onboard Kalman filter orbit determination algorithms to converge after initialization. Therefore, the results for this period have not been included in the tables and plots presented in the following section.

Observations

The measurement interval was fixed at 30 s, in which both the chaser and the target acquire one observation of each visible GPS satellite. This was done to limit the total number of observations to be processed during the analyses. In practice, measurements will probably be made every second or even faster. To compensate for this, the measurement precision was increased by a factor of $\sqrt{30}$. A nominal cutoff elevation angle of 10 deg was adopted with respect to the local horizons of the individual spacecraft.

The measurement precision of the pseudorange observations depends on the receiver electronics and also on the code frequency of the GPS signals. Although the best ground receivers today achieve a precision of about 1 m for S-code pseudorange measurements, in this study a conservative value of 10 m was adopted. It is representative of the performance of a relatively simple receiver being studied for the operational orbit determination of CFFL.[11] When using single differences as data type, a measurement precision of $\sqrt{2}$ times the nominal value is used, assuming that the noise errors of the receivers onboard the chaser and target are uncorrelated. This makes it possible to compare the results obtained with these two different data types.

The effects of SA were not considered in this study. It is well understood how it affects the observations, and, therefore, it can be safely assumed that the effects will largely cancel in the relative positioning solutions. The same applies for the ionospheric propagation effects, which were also neglected because the simulation software was not able to model them.

Of course, there is another data type that is obviously highly attractive for application to GPS-guided rendezvous, namely, carrier phase. Experiences with ground-based receivers suggest[12] that using that kind of data in combination with pseudorange would probably make it possible to achieve subdecimeter relative position accuracy over large distances. However, it was beyond the scope of this study to investigate this. Still, to get an impression of the potential improvements due to the application of highly precise measurements, an extra analysis was performed using 10-cm precision P-code measurements, which may be within the capabilities of a future generation GPS receiver.

Error Model

It was already mentioned that for onboard real-time navigation only a simple dynamic model will be applied in the filter algorithms, to limit the computational effort. For the analyses it has been assumed that the gravity model will only contain terms up to degree and order 4. To simulate the errors due to the unmodeled higher order part of the "real" gravity field, all terms between deg 5–8 were treated as consider parameters, with the values of their coefficients according to Kaula's rule.[13] Although this error model only partially accounts for the total uncertainties caused by the omission of most of the gravity field, it is felt that it may still provide a rough first impression of the effects to be expected from this error source. In general, the lowest-degree terms cause the largest perturbations. Another significant error source will be drag. The discrepancies between some simple model, used in the hypothetical onboard filter, and the "real" drag force have been accounted for by applying a drag error of 10% of the modeled effect. All other perturbations, such as luni-solar attraction, are assumed to be modeled perfectly in the onboard filter algorithms, or the remaining discrepancies are considered to be negligible with respect to the other error sources.

The other elements of the error model are the GPS satellite ephemerides and clock offsets. It is assumed that these parameters will not be adjusted by the relative navigation software, but that they are treated as constants. This information, which is updated every hour, is extracted from the navigation messages broadcast by the GPS satellites. When SA is not active, the uncertainties are estimated to amount to 10 m in each position component, 1 mm/s in each velocity component, and 10 ns for the clock offset, averaged over a 12-h period. With SA on, the uncertainties will be about three times larger. These errors were modeled as seven independent consider parameters for each of the 18 GPS satellites. It is emphasized that the ephemeris errors are modeled as biases in the state vectors of the GPS satellites at a reference epoch, the effect of which is propagated to the observation times. This means that they are not uncorrelated from observation time to observation time. However, it is well known that the uncertainties in the individual components of each state vector are highly correlated. Therefore, it would have been better if they could have been specified in orbital element space. Since this was beyond the capabilities of the software, the effect of the GPS ephemeris errors on the absolute navigation accuracy may be considerably exaggerated. Fortunately, the ephemeris errors largely cancel out in relative navigation problems.

State Parameters

The total number of state parameters, estimated for each of the two rendezvous spacecraft, is 10. They include the six inertial position and velocity components, one receiver clock bias, and the three acceleration components associated with the reduced-dynamic estimation approach described previously. It was assumed that both receivers utilize quartz clocks with a typical stability of 10^{-9}. This has been modeled by treating the clock biases as random walk processes. The accelerations, which represent dynamic process noise, were modeled as first-order exponentially time-correlated Gauss-Markov processes with a steady-state sigma σ_p of 1.0 μm/s^2 and a correlation time τ equal to the initial orbital period of the chaser and the target ($\sim$90 min). This particular value for τ was selected because the errors due to dynamic mismodeling are known to have a dominant frequency of one cycle per revolution. The value of the steady-state sigma is consistent with the magnitude of the perturbing accelerations of the unmodeled part of the forces acting on the satellites.

The main characteristics of the overall analysis model are summarized in Table 2.

Table 2 Measurement parameters and nominal error model

Measurements	
Data type	Pseudoranges
Data noise	10 m (and 0.1 m for special test)
Data rate	1 observation to each GPS per second
Cutoff elevation	10 deg
Ionospheric refraction	Not modeled/considered
Adjusted parameters	
Chaser/target state vector	Free adjustment
Chaser/target clock	Random walk with 10^{-9} stability
Chaser/target accelerations	Process noise with 90-min correlation time and 1.0-μm/s^2 steady-state sigma
Consider parameters	
Geopotential error	All terms of deg 5–8; coefficients according to Kaula's rule
Atmospheric drag error	10% of the effect
GPS epoch state-vectors	10 m (x, y, z); 1 mm/s ($\dot{x}, \dot{y}, \dot{z}$)
GPS clock offsets	10 ns

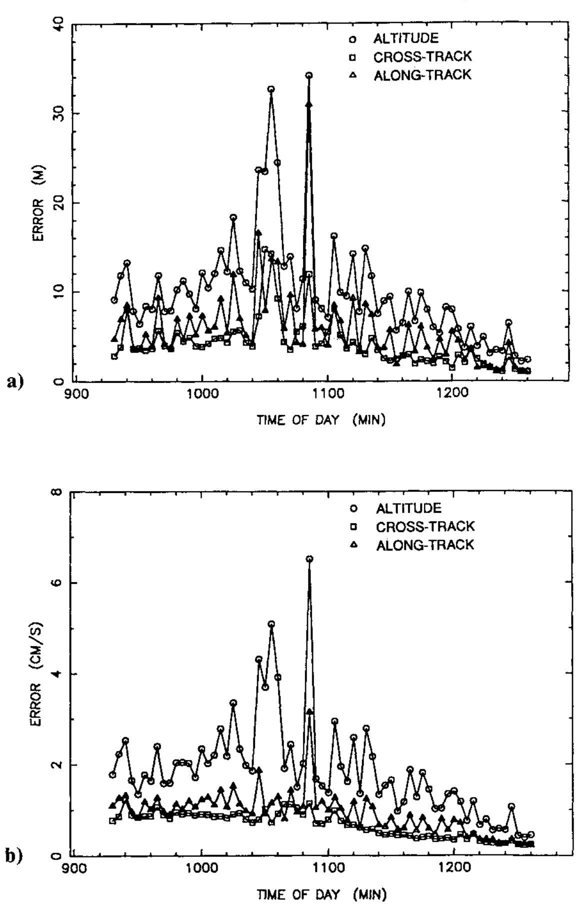

Fig. 3 The variation of the total errors in the a) relative position and b) velocity components for the nominal case, using undifferenced S-code pseudorange observations.

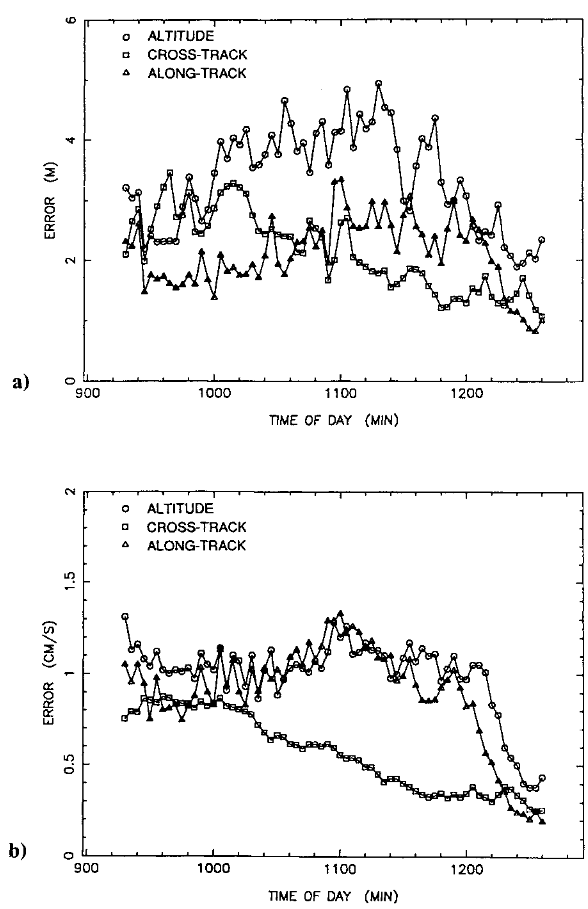

Fig. 4 The variation of the total errors in the a) relative position and b) velocity components for the nominal case, using S-code single difference observations.

Table 3 Summary of the average total errors in relative position and velocity for the different analyses

Error model	Measurement type	Position error, m			Velocity error, cm		
		Altitude	Cross	Along	Altitude	Cross	Along
Nominal	S-code pseudorange	11.9	5.0	7.2	2.1	0.7	1.0
Nominal	S-code single difference	3.4	2.2	2.2	1.0	0.6	0.9
Data gap	S-code single difference	13.7	3.1	62.7	7.0	0.6	1.7
9 GPS	S-code single difference	11.2	7.1	10.2	1.9	0.7	2.0
Elevation 20	S-code single difference	4.1	2.5	2.4	1.0	0.6	1.0
Elevation 30	S-code single difference	4.8	3.0	2.9	1.0	0.6	1.0
Nominal	High-precision single difference	2.4	0.9	1.1	0.7	0.7	0.7

Results of the Covariance Error Analyses

In this section, the results of the analyses based on the previously described nominal model will be presented first, discussing the accuracies achieved for both undifferenced and single-difference S-code measurements. Subsequently, four additional analyses will be discussed in which the effects of equipment failures and reduced visibility of GPS satellites were investigated. They should be considered as crude attempts to simulate some of the problems that may occur in real operations. The investigated problems include a loss of tracking data during one revolution of the LEO satellites, a total failure of half of the GPS satellites, and two cases with a higher cutoff elevation angle to simulate nonhemispherical antenna coverage, for example, due to attitude changes or partial obstruction. These four analyses were only performed for S-code single-difference observations. Finally, the results of an analysis using extremely precise P-code single differences are discussed. All results are presented as relative position and velocity errors in altitude, cross-track, and along-track components, defined in a corotating reference frame with its origin at the center of gravity of the target.

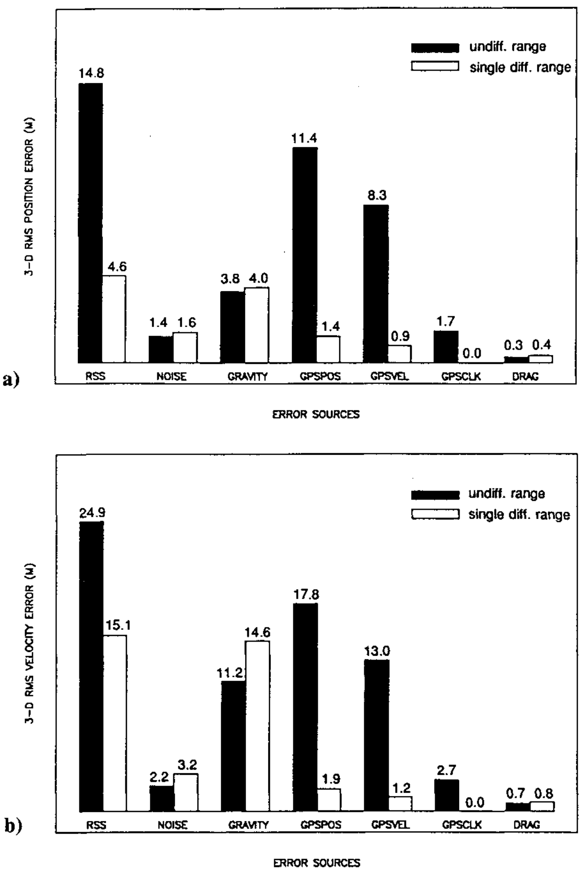

Fig. 5 Comparison of the contributions of the individual error sources to the total three-dimensional a) relative position and b) velocity errors, using undifferenced (solid bars) vs differenced ranges (open bars).

Results for the Nominal Model

In Fig. 3, the total errors in the position and velocity components, as obtained from the analysis with the nominal model and using undifferenced pseudoranges, are plotted as a function of time. The total error is defined as the root-sum-square (rss) of the contributions of all error sources. Note that the distance between the two spacecraft decreases as the time increases. The plots show that during most of the time the errors remain relatively constant, at a level of 2–15 m for the position components and 0.5–2.5 cm/s for the velocity. Only near the end, when the chaser closes in on the target, is there a tendency for the errors to become smaller. The explanation is that since the GPS satellites are at an altitude of 20,000 km, whereas the rendezvous spacecraft are at 500 km and less than 1000 km apart, the errors, due to the nondynamic error sources like GPS ephemerides and clocks, will affect the measurements of both receivers almost identically and lead to similar errors in the absolute navigation solutions of both satellites. When these are differenced to obtain the relative navigation solution, these errors will largely cancel, except for a small residual differential error caused by the slightly different observation geometries. This cancellation effect becomes stronger as the distance between the satellites diminishes. It is not so pronounced in Fig. 3, because the ephemeris errors of the GPS satellites are growing at the same time, which makes the residual differential errors increase. The total number of measurements in the 6-h data period was 7504.

The most remarkable features are the spikes in the plots. They are caused by the relative changes in the GPS constellations observed by each of the satellites. This can be seen as follows. Because of the relatively large distance between chaser and target during the first phase of the mission, a particular GPS satellite may still be in view from the chaser, for example, while it is already below the cutoff elevation of the target. This means that the absolute navigation solutions of the two spacecraft are temporarily based on different sets of observations. As a consequence, the errors caused by the odd GPS satellite will not cancel in the relative solution. Instead, the full effect of these errors will come to expression, as demonstrated by the spikes. Most of it is obviously corrected again as soon as the symmetry of the tracked GPS constellations is restored. The spikes are relatively large because the GPS ephemeris error model overestimates the uncertainties, especially after a time span of more than one revolution of the LEO satellites. The reason for this was explained in the section describing the error models.

The corresponding results for single-difference observations are plotted in Fig. 4. The total number of measurements for this case was 3582. This is slightly less than half the number of pseudoranges of the previous analysis. The reason it is not exactly half is that single differences can only be formed from simultaneous observations of the same GPS satellite by both chaser and target. It has just been pointed out, however, that the observed GPS constellations are not always identical for both satellites. (If they are in opposite hemispheres, there is no common visibility at all!) Therefore, some of the observations cannot be used to create single differences. So, since only measurements from commonly observed GPS satellites are used, the largest part of the common errors always cancels in the differencing. For this reason, the spikes are absent in the results of this analysis. This could also have been achieved in the previous analysis if only the pseudorange measurements from the commonly observed GPS satellites would have been processed. However, due to current software limitations, this experiment could not be carried out.

From Fig. 4, it can be seen that the average overall errors have decreased to a range of 1–5 m in the position components and to a level of 0.2–1.3 cm/s for the velocity. These are about half the values of the undifferenced case, if the effect of the spikes is neglected. This is curious, since, intuitively, one would expect these results to be about the same. However, there is apparently a difference between simultaneous orbit determination of two spacecraft from single-difference observations and individual orbit determination from undifferenced observations. It can be shown that, from a mathematical point of view, the two methods are indeed not identical. In the first method, both satellite state vectors are estimated from the same differenced measurements, which causes cross correlations between them and, therefore, also affects the covariance matrices of the individual satellites. This is not the case for the other method, where the cross correlations are zero. Through the sensitivities, which are also a function of the state covariance matrices, this leads to a different propagation of the model errors for the two methods. The physical explanation is that, due to the lack of absolute scale in the difference measurements, the orbits have more freedom to adjust than in the undifferenced case. This may lead to poorer orbit estimates with larger absolute errors, but these combine to smaller relative errors than in the case with undifferenced measurements.

The difference in the results of the two methods is further detailed in Fig. 5, where the effects of groups of individual error sources on the relative navigation accuracy have been summarized in two histograms. The height of each column represents the rss of the total three-dimensional position or velocity error, due to a group of error sources, over the entire analysis period. The figure clearly shows that the errors due to uncertainties in the GPS position and velocity components and the clocks are much smaller when the single-difference method is used. Although this is partially caused by the effects of the spikes in the undifferenced case, the improvement is still significant when these effects are eliminated. The errors due to data noise and dynamic mismodeling appear to be slightly larger for the single-difference case. This can be explained from the small loss of measurement information, which is incurred during the creation of the single differences, as was pointed out previously. Overall, their contribution remains at the same level, however, demonstrating that the common estimation of both satellite orbits from single differences is not effective to reduce the differential effects of the dynamic model errors. It is interesting to note that the relative position errors due to data noise are much smaller than the data noise itself. This means that the reduced-dynamic technique has been successful in dynamically coupling the observations, while at the same time limiting the errors due to the other error sources, which would otherwise have grown without bound.

From the comparison of these two analyses, it is concluded that the use of single-difference measurements has two advantages. First, perfect observation commonality is implied, optimizing the cancellation of common errors. In the second place, it allows simultaneous orbit determination of both satellites, which reduces the errors due to the nondynamic error sources even further. As a consequence, all other analyses in this study are based on single differences only.

Data Gap

It is conceivable that, in real operations, the tracking of the GPS signals by either or both of the rendezvous spacecraft is interrupted. To investigate the consequences of such an event, an analysis was performed in which a 1.5-h data gap was introduced starting at the beginning of the second revolution after the maneuver. This reduced the total number of single-difference observations to 2658. The results are plotted in Fig. 6, which shows the variation of the total rms errors in the relative position components, due to the combined effects of all error sources. During the interruption, the along-track component runs off scale to a maximum of about 200 m. This is primarily caused by the errors in the dynamic model, used to propagate the state-vector solutions of the chaser and the target, obtained just before the gap. Taking into account the relatively low altitude of the satellites in combination with the severe gravity field mismodeling, this is a remarkably good result, especially when compared with the absolute position errors, which become much larger (up to 2.2 km in 2 h), as is shown in Ref. 3. The explanation is that the gravity field errors affect the orbits of both satellites quite similarly, because they are relatively close with respect to the dimensions of the Earth. Therefore, the largest part of the effect also cancels in the relative position. As soon as the tracking resumes, the relative position errors return to the same level as before the interruption.

Degraded GPS Constellation

In another analysis the effects of a severe degradation of the GPS constellation was considered. This was done by eliminating one or two GPS satellites out of each orbital plane, so that only nine remained. This is an arbitrary but rather severe

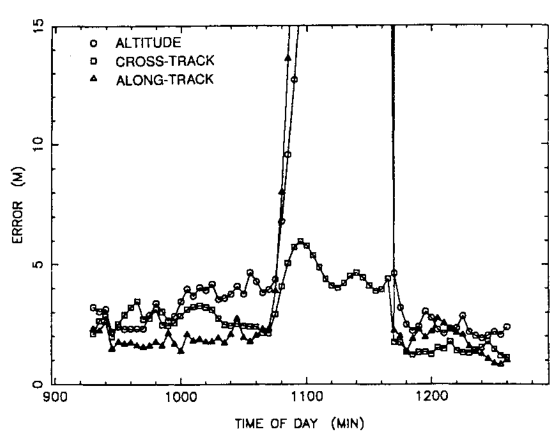

Fig. 6 The variation of the total errors in the relative position components for the case with a 90-min data gap.

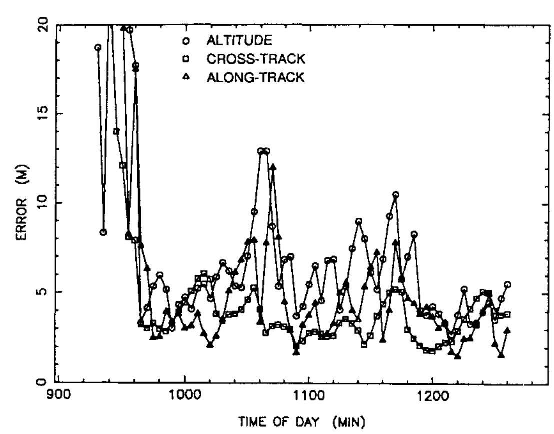

Fig. 7 The variation of the overall errors in the relative position components for the case with a GPS constellation reduced to nine satellites.

failure model, although the elimination of all satellites in one hemisphere would have been worse. From the observations of the nine remaining GPS satellites, only 1733 single differences could be formed. The results are presented in Fig. 7. It is evident that this time the filter solutions have not yet converged in the half hour preceding the start of the plot, due to the lack of sufficient observations. However, after another half hour, the errors stabilize at about the 5-m level. Of course, this is worse than for the nominal case by about a factor of 2, but it is still more than sufficient to allow a safe approach between the two spacecraft.

Reduced Visibility

To assess the effects of a partial blocking of the field of view of the GPS antennas onboard the rendezvous spacecraft, two additional analyses were performed. In real operations, the antenna coverage may be reduced due to attitude maneuvers. This can easily occur for a satellite-fixed antenna with a hemispherical field of view. If such an antenna is tilted, some GPS satellites may disappear below the horizon of its field of view, causing a loss of tracking data. Another possibility is that part of the field of view is obstructed by the other spacecraft, which may occur during the final phases of the approach. The only practical way this could be simulated was by increasing the cutoff elevation angle. This was done for the chaser, since this is the maneuvering element during the rendezvous. The analyses were performed using two different values for the cutoff elevation of 20 and 30 deg. This reduced the mean number of visible GPS satellites from five in the nominal case to four and three, respectively. At the same time the number of single-difference observations dropped to 2883 and 2117, respectively. Nevertheless, the results appear to be quite similar to those of the nominal case, except that the mean errors are slightly larger. This is shown in Table 3, where the results are summarized, together with those of all of the other analyses. It demonstrates again that accurate relative navigation for rendezvous using GPS is quite feasible, even under degraded conditions.

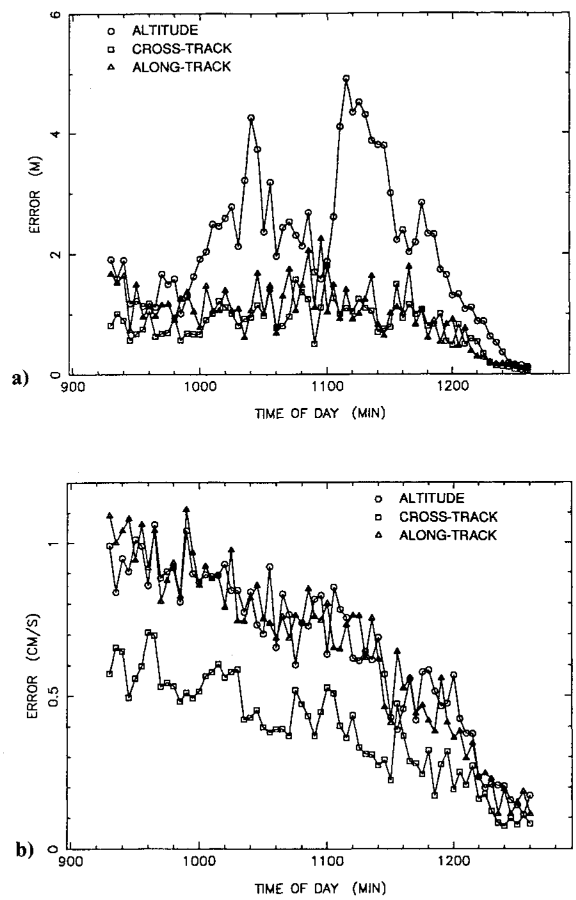

Fig. 8 The variation of the total errors in the a) relative position and b) velocity components for the nominal case, using high-precision single difference observations.

High-Precision Measurements

To complete this study, a final analysis was performed to investigate the use of extremely precise observations. For this purpose the nominal case was reanalyzed using single-difference observations with a data noise level 100 times lower than that of the S-code measurements. This corresponds to a measurement precision of 10 cm (at a rate of 1 observation per second), which is between the subcentimeter level of the carrier phase observations of current state-of-the-art geodetic receivers and 50-cm P-code noise, which is also within reach of today's technology.

Figure 8 shows the results for the total errors in the relative position and velocity components. The mean position errors appear to be about half as large as for the nominal case, but the peaks in the altitude component are still of the same magnitude. It was found that they are primarily caused by the GPS ephemeris errors, which are now the dominating error source. The reason is that, due to the high precision of the measurements, the relative weight of the geometric error sources increases. With the same tuning of the parameters controlling the reduced-dynamic technique, the balance has shifted further toward the geometric information. This leads to larger contributions from these error sources, whereas the dynamic errors decrease.

In particular, the altitude component is apparently very sensitive to the GPS ephemeris errors. The largest uncertainties occur during the phase when the satellites are still relatively far apart. However, as the chaser and target move closer, the errors in the absolute position of the individual satellites become more similar, so that they cancel in large part in the relative position solution. This phenomenon is dramatically demonstrated in the plot, which shows that the errors fall off strongly toward the end. Ultimately, this results in relative position errors of only 10 cm, which is at the data noise level. The relative velocity errors, also depicted in Fig. 8, appear to decrease continuously until they reach a level of 0.1 cm/s at the end. From these results, it can be concluded that it might even be feasible to perform (automatic) docking under control of a navigation system based on GPS tracking, provided that both spacecraft are equipped with sufficiently accurate GPS receivers. The main problem will be to guarantee the integrity of the system.

Summary of the Results

The results of all the computations are summarized in Table 3. It lists the average values (rss) of the total errors over the 5.5-h time span following the initialization of the filter solution in the first half hour of the analyses. The main thing to be noted is that the accuracy of all solutions, except for the case with the data gap, is better than what can be achieved with instantaneous relative positioning. In that case, assuming a geometric dilution of precision factor (GDOP) of 3, the position uncertainty due to data noise only would have been about 25 m in each component. Considering the fact that there are many other error sources and that the numbers in the table are averages over the whole mission, this is a remarkable result. It is a demonstration of the effectiveness of the reduced-dynamic technique. The results compare favorably with those presented in Ref. 7, where white noise was added to the filter covariances. Taking into account the differences in the error models, there is a factor 3–4 improvement, which becomes even larger when only the final phase of the approach is considered.

It was found that gravity mismodeling is the major error source for all cases utilizing single-difference observations.

With undifferenced pseudoranges, the GPS ephemeris errors dominate. Drag mismodeling hardly appears to affect the accuracy of the solutions. It is apparently effectively absorbed by the stochastic acceleration parameters.

Conclusions

A covariance error analysis of the performance of a hypothetical GPS based real-time relative navigation system for a rendezvous mission between the European spaceplane Hermes and the Columbus Free Flying Laboratory has been presented. The applied error model included simplified representations of nondynamic as well as dynamic error sources, such as the gravity field, drag, and GPS ephemerides. Furthermore, the effects of failures and degraded tracking capabilities were investigated. The onboard navigation software was assumed to employ a Kalman filter for the processing of the GPS observations. To allow the use of simple dynamic models, the so-called reduced-dynamic technique was applied, in which three additional adjusted acceleration parameters are modeled as process noise. Two different data processing concepts, involving differential navigation and simultaneous orbit determination from differenced observations, were investigated.

It was shown that the accuracy of the differential solution, based on absolute S-code pseudorange measurements, varies from 2 to 35 m in the position components and from 0.5 to 7 cm/s for the velocity. These results improved considerably when perfect commonality between the GPS observations processed from both rendezvous spacecraft was enforced. This was demonstrated by processing the same observations as single differences. In that case the relative position errors reduced to between 1–5 m and between 0.2–1 cm/s for the velocity. It was found that the improvements achieved with this technique are even larger, because the correlations between the state vectors, which come about automatically, reduce the effects of the nondynamic errors still further. Also, the reduced-dynamic technique seems to offer a better performance than the standard technique of adding white noise to the filter covariance matrix in order to stabilize the filter. To apply this technique in practice, it is only required that the observations acquired by the GPS receiver onboard the target are transmitted to the chaser. There, a relatively simple computer algorithm, based on the reduced-dynamic technique, can then be used to compute the orbits of both satellites simultaneously, or the equations for the relative motion may be solved directly.

It has also been shown that, during a 1.5-h interruption of the data stream from the GPS receivers in the middle of the mission, the relative position solution can still be propagated with a maximum uncertainty of about 200 m in the along-track component at the end of the break. This is quite sufficient to continue safe operations under such conditions. It only requires that the filter solution has converged before the break occurs. Furthermore, it has been demonstrated that, even when the tracking capabilities are severely degraded—for example, due to failure of GPS satellites or obstructions in the antenna field of view—the performance is hardly affected. A degradation by a factor of 2 may occur, but in view of the high basic accuracy, this is quite acceptable for the major part of the rendezvous mission.

Only the final approach phase requires better accuracy, but then the precision of the S-code measurements becomes the limiting factor. However, this problem may be solved by using the much more precise carrier phase observations in addition to S-code or P-code pseudorange observations. This was demonstrated by a special analysis in which 10-cm precision pseudoranges were processed as single differences. The average relative position errors were found to be reduced by a factor of 5 during the major part of the mission. Even more significant is the fact that during closest approach the errors are down to the data noise level of about 10 cm. This would mean that even (automatic) docking could be performed under control of a GPS navigation system.

Summarizing, the results of the covariance error analyses presented in this paper seem to indicate that GPS can be extremely useful for the navigation of rendezvous missions. However, many aspects still need to be investigated further. In particular, the error model can be improved and expanded to include ionospheric propagation errors and perturbations due to thruster operations. Furthermore, the application of carrier phase measurements deserves more attention, and it would be interesting to see an honest comparison with kinematic techniques based on this kind of data, not just in terms of performance, but also from the point of view of system integrity. Finally, it would be very helpful to obtain some experimental data of a space-borne GPS receiver in order to obtain a better characterization of the performance and the error model of such a system. It would also allow a verification of the results of covariance error analyses as carried out in this study.

References

[1]Caldichoury, M., Champetier, C., and Desplats, E., "Hermes Rendez-Vous with the Space Station," *Proceedings of the 1989 AGARD Conference on Space Vehicle Flight Mechanics* (Luxemberg), No. 489, Nov. 1989, pp. 14-1–14-21.

[2]Snijders, R. J., "Rendez-vous & Docking Using the NAVSTAR Global Positioning System (GPS)," Technical Thesis, Faculty of Aerospace Engineering, Delft Univ. of Technology, Delft, The Netherlands, Sept. 1989.

[3]Hesper, E. T., Ambrosius, B.A.C., Leenman, H., and Wakker, K. F., "Hermes Navigation/Localization GPS/DRS Simulations," Delft Univ. of Technology, Faculty of Aerospace Engineering, Final Rept., ESA Contract 5E.593.01.E, Delft, The Netherlands, April 1989.

[4]Matchett, G., "GPS-Aided Space Shuttle Navigation," *Proceedings of the 1978 National Aerospace and Electronics Conference* (Dayton, OH), Inst. of Electrical and Electronics Engineers, New York, Vol. 1, May 1978, pp. 292–300.

[5]Okkes, R. W., and Lucas, R., "GPS Relative Navigation for Space Vehicles," *Proceedings of the International Technical Meeting GPS Around the World* (Washington, DC), 1989, pp. 89–93.

[6]Martinez, M. A., Perez, M., and Lucas, R., "GPS Navigational Performance in Space Rendez-Vous Operations," *Proceedings of the 2nd European In-Orbit Operations Technology Symposium* (Toulouse, France), European Space Agency, Noordwijk, The Netherlands, Sept. 1989, pp. 227–235.

[7]Axelrad, P., and Kelly, J., "Near-Earth Orbit Determination and Rendez-Vouz Navigation Using GPS," *Proceedings of the 1986 Symposium on Position Location and Navigation* (Las Vegas, NV), Inst. of Electrical and Electronics Engineers, New York, Nov. 1986, pp. 184–191.

[8]Wu, S. C., Yunck, T. P., and Thornton, C. L., "Reduced-Dynamic Technique for Precise Orbit Determination of Low Earth Satellites," AAS/AIAA Astrodynamics Specialist Conference, Kalispell, MT, Aug. 1987 (AAS Paper 87-410).

[9]Wu, S. C., Border, J. S., Lichten, S. M., Sunseri, R. F., Williams, B. G., and Wu, J. T., *OASIS Users' Guide,* Vol. 1.0, D-3138, Jet Propulsion Lab., California Inst. of Technology, Pasadena, CA, April 1986.

[10]Hesper, E. T., "Mathematical Description of the Real Time Relative Orbit Determination of Two Space Vehicles Using the OASIS System," Delft Univ. of Technology, Faculty of Aerospace Engineering, LR-649, Delft, The Netherlands, Jan. 1990.

[11]Lucas, R., Martin-Neira, M., Bethmann, A., Llorente, J. S., "GPS Activities Overview at ESA/ESTEC," GPS Technical Interchange Meeting, NASA/Johnson Space Center, Houston, TX, Nov. 1990; based on "GPS Receiver and Processor Unit Predevelopment," ESA Contract 8339/89/NL, June 1992.

[12]Blewitt, G., "Carrier Phase Ambiguity Resolution for the Global Positioning System Applied to Geodetic Baselines up to 2000 km," *Journal of Geophysical Research*, Vol. 94, No. B4, 1989, pp. 3949–3966.

[13]Kaula, W. M., *Theory of Satellite Geodesy,* Inst. of Geophysics and Planetary Physics, Univ. of California at Los Angeles, Blaisdell, Waltham, MA, 1966.